LA-UR- 99-2528

Approved for public release;
distribution is unlimited.

Title: SEISMIC ANALYSIS OF A FIRE LOOP PIPING SYSTEM

Author(s): John E. Crawford, Karagozian & Case Structural Engineers, Glendale, CA
Carl J. Costantino, City College of Engineering, NYC, NY
Lawrence K. Goen, ESA-EA
Douglas E. Volkman, PM-2

Submitted to: 1999 ASME Pressure Vessels and Piping Conference
Boston, MA, August 1-5, 1999

SEISMIC ANALYSIS OF A FIRE LOOP PIPING SYSTEM

J. E. Crawford
President, Karagozian & Case Structural Engineers,
Glendale, CA, USA

C. J. Costantino
Professor, Dept. of Civil Engineering, City College of New York
New York, NY, USA

L. K. Goen, Project Leader for Seismic Studies
D. Volkman, Seismic Coordinator
Los Alamos National Laboratory

ABSTRACT

This paper summarizes the studies conducted to assess the seismic capability of a fire loop piping system that is being installed at the Los Alamos National Laboratory (LANL) to serve a series of critical facilities. The approach used in the evaluation was to develop a complete finite element model of the entire fire loop piping system and its appurtenances external to the structures being protected. The seismic loading was input to this system in the form of specified accelerograms selected to match given response spectral criteria. The system responses were then computed using the ADINA nonlinear finite element program, incorporating several nonlinear aspects relating to pipe-soil interaction and pipe bending. A series of calculations were performed to assess the effects of direction of the seismic input, potential variability in site parameters as well as materials of the piping system. Calculations of response were performed for both ductile iron (DI) and high-density polyethylene (HDPE) pipe.

INTRODUCTION

The fire loop piping system protecting a series of critical facilities at the LANL is in the process of being upgraded and seismically qualified. The piping system consists of buried piping surrounding the facilities, as shown in Fig. 1, risers to hydrants and into the buildings, water storage tanks and pumping facilities. This paper describes the analyses used in the design and analysis of the piping system. An attempt was made to account for the uncertainties associated with the direction of potential seismic ground motion as well as site soil and piping stiffness properties. The approach taken was to develop a complete finite element model of the fire loop piping system, including risers and hydrants and all the pertinent components that relate to seismic loading. The ADINA computer code was used to assess the time dependent system responses, incorporating nonlinear aspects of the problem into the analysis; such as, the potential for longitudinal slip of the pipe with respect to the soil, different vertical stiffnesses in the up/down directions and the effect of pipe ovalling on bending stiffness. Calculations were performed using soil parameters that were varied from best estimate to upper/lower bound values. Pipe stresses were calculated at over 1,000 points of the fire loop, including every tee, elbow and building interface and peak demand/capacity ratios computed for each case.

LOOP MODEL

ADINA (1995) is a general-purpose nonlinear finite element computer code developed at MIT (Bathe, 1982). The code contains a library of element types and material models along with a variety of special features, including loading and solver options. For these computations, a step-by-step transient solution of the equations of motion was obtained using an implicit Newmark operator. The integration time step was made small enough to adequately approximate the wave speeds across the site and capture the maximum pipe frequencies of interest. Typically, a time step of about 5 milliseconds was found adequate for these analyses.

The fire loop pipe was modeled as either high-density polyethylene (HDPE) pipe having an elastic modulus of 130 ksi or ductile iron (DI) pipe with an elastic modulus of 24,000 ksi. Pipe diameters varied from a minimum of about 6.5" to about 11" in the pipe loop. For the HDPE pipe analyses, short lengths of DI pipe were used to connect the loop into the buildings. All of the piping of the loop was modeled using over 1,100 Hermitian beam elements. A sample of the discretized loop is shown in Fig. 2. The weight of the pipe and the water inside were combined to determine pipe element mass. The hydrants were included in the model by adding a pipe stem and mass at the point in the piping where the hydrant was attached. Pipe-soil interaction was included along the stem but omitted at the top of the riser.

The connection of the fire loop to each building was modeled by individually assessing the stiffness of the surrounding soil and/or grout placed at the building entrance. For each seismic motion considered, the motion of each building was first computed individually, using a simple stick model of the building together with simple interaction coefficients determined from constant impedance functions (ASCE Std 4, 1996). The translational DOF's of the piping nodes at the building entrance were then given the same horizontal and vertical motion as the individual building. Rotational DOF's were kept fixed. Relative building displacements were found to be only of the order of 1% of the free-field motion. The assumption of moving the building with the free-field is therefore a reasonable one.

SOIL MODELS

A variety of soil conditions exist along the path of the fire loop as determined from a series of shallow borings taken at a number of locations along the loop (Keller, 1997). The soils consist of either recently placed fill or in-situ tuff of varying properties, depending upon the welded characteristics of the tuff. The pipe trench, which is 3' wide and of variable depth, is to be backfilled by a clean sand backfill placed at optimum compaction. The pipe is located in the center of the trench on a 1' thick bed of backfill. The surface fill material at the site consists of a variety of clayey and silty sands which overly the in-situ tuff. At a few locations, the entire trench will be located in the tuff materials. The best estimate elastic properties for the various soils along the pipe loop are given in Table 1. Upper and lower bound values for each of the stiffness parameters were estimated based upon measured variability in SPT sample blow count, data available from a number of site specific geotechnical reports or using normal variability estimates recommended for such analyses (ASCE 4, 1996). Typical potential variability assumed in the elastic properties is indicated in Table 2 for the case of P-wave velocities.

PIPE-SOIL INTERACTION MODELS

Pipe-soil interaction stiffnesses are required in both orthogonal and parallel directions to the pipe centerline. The effect of the soil-pipe interaction is modeled in the analysis by spring coefficients as shown in Fig. 3. For directions orthogonal to the pipe centerline, pipe-soil stiffnesses were derived using static finite element models as indicated in Fig. 4. Typical pipe-soil cross-sections fall into three categories; namely, a cross-section where the trench lies entirely in in-situ tuff, one in which the trench lies entirely in fill and a third where the tuff/fill interface is about at the level of the pipe. For each profile type, as defined by the available boring data, spring constants were developed in the horizontal and both vertical (up and down) directions from these static FE analyses.

For motion parallel to the pipe centerline, estimates of the spring coefficients were obtained from out-of-plane static analyses of the pipe-soil FE models, assuming that free-field displacements are applied to the trench boundaries. Peak friction forces were then estimated by assuming simple Coulomb friction values based on the average confining pressures developed along the pipe. For values of friction less than the peak values, the friction force developed along the pipe was computed from the spring coefficient. For values exceeding the peak values, the soil was allowed to slip past the pipe and only the peak friction force transmitted to the pipe. Again, computations were made for a range of values of friction force coefficients varying from 0.3 to 0.5.

SEISMIC FREE-FIELD INPUT MOTIONS

The design of the piping system is intended to satisfy the seismic criteria defined by Department of Energy (DOE) and LANL design guides (Goen, 1995) and provide safety margin against failure associated with Performance Category 3 criteria (DOE Standard 1024). The site-wide seismic criteria associated with the PC3 category is defined by the 5% damped acceleration response spectrum as shown in Fig. 5 for both horizontal and vertical seismic motions. The peak design acceleration is 0.31g in the horizontal direction and 0.29g in the vertical direction. The peak spectral amplification of the 5% damped spectrum is 2.39 in the horizontal direction and 2.83 in the vertical direction.

A series of horizontal accelerograms were developed which match the 5% damped horizontal response spectra and which defines the seismic environment. These motions were developed using the CARES computer code (Costantino, et al, 1996). The characteristics of the developed accelerograms are such that they have a peak acceleration which equals the target value, closely matches the specific spectrum (in the sense of the US NRC Standard Review Plan, 1989) and provides a total strong motion duration appropriate for the earthquakes comprising the LANL seismic hazard. Both random and earthquake-specific Fourier spectra phasing were used to generate the various motions used in the study. Similar motions were developed which match the vertical spectrum. A comparison of the spectra from the individual accelerograms with the target spectrum is shown in Figures 6 and 7 for the horizontal and vertical cases. A typical time history is shown in Fig. 8 with a total duration of about 18 seconds, a peak acceleration of 0.31g, a peak velocity of about 12 inches per second and a peak displacement of about 5 inches. This motion was developed assuming the earthquake was a magnitude 7 event. Motions were developed which are considered appropriate for both magnitude 6.5 and 7.0 events.

For each problem analyzed, ground motion sets (two horizontal and one vertical) were selected from all the motions available which were then used as the definition of the free-field input motions to the FE model. These motions were propagated across the site at a best estimate uniform velocity of 3,000 fps in a given direction or azimuth. A total of eight different directions of ground motion were used in the evaluations as indicated in Fig. 1. In addition, the influence of the variation in propagation wave velocity was accounted for by obtaining solutions using free-field wave speeds of 2,000 fps and infinite (i.e., the motions are applied at the same time at all ground nodes of the pipe loop).

PIPE CAPACITY ESTIMATES

A requirement that is generally imposed on buried piping complies with the ASME B31.1 recommendation that classifies earthquake loading as an occasional load. As such, seismic loads are subject to the stress criterion for longitudinal stress given by:

$$\frac{P D_0}{4 t_n} + \frac{0.75 i M_A}{Z} + \frac{0.75 i M_B}{Z} < k S_h \qquad (1)$$

where M_A is the resultant moment loading on a cross-section due to weight and other sustained loads, M_B is the resultant moment on the cross-section due to occasional loads, Z is the section modulus, i is the stress intensification factor, and k is a factor which is 1.15 for occasional loads acting for less than 10% of any 24 hour period and equal to 1.2 for occasional loads acting less than 1% of any 24 hour operating period.

Goodling (1982) recommends a modification to the above equation by noting that, in general, M_A is about 0 for buried pipelines but then includes effects of axial stress due to the earthquake. Equation 1 then becomes

$$\frac{P D_0}{4 t_n} + \frac{F}{A} + \frac{0.75 i M_B}{Z} < k S_h \qquad (2)$$

where F is the axial load due to earthquake and A is the cross-sectional area of the pipe.

The stress intensification factor is included to account for stress concentration effects in fittings such as elbows and tees due to ovalling during bending. Computation of this factor first involves the computation of the fitting flexibility factor, h, which for a 90• bend is

$$h = \frac{tR}{r^2} \qquad (3)$$

where t is the wall thickness, R is the bend radius and r is the inside radius of the fitting. The corresponding factor for a tee is

$$h = \frac{t}{r} \qquad (4)$$

The stress intensification factor can then be found for either fitting by the relationship

$$i = \frac{0.9}{h^{2/3}} \qquad (5)$$

The factors discussed above and presented in B31.1 are defined for metal pipe bends and junctions. Antaki (1997) in evaluations of test data for HDPE piping recommends that these factors are still appropriate for this material.

The value of S_H in equation 2 is the basic material allowable stress at maximum operating temperature. For DI pipes, this value is defined as the lower of:

- One-fifth the minimum tensile stress at room temperature, or
- One-fifth the tensile strength at operating temperature.

For A536 Grade 60-42-10 Pressure Class 350 DI, v is 12,000 psi. For thermoplastic materials, this value is limited to one-half the hydrostatic design basis at the design temperature as determined by test data. For HDPE pipe, the hydrostatic design basis is 1,600 psi and the hydrostatic design stress is 800 psi.

Antaki (1997) suggests a somewhat different stress criterion than equation 2 that is based on the ultimate strength of the pipe material, or

$$\nu \frac{P D}{2 t} + \eta \frac{F}{A} + \frac{i M}{Z} < \frac{S_u}{SF} \qquad (6)$$

where ν is Poisson's ratio of the material, P is the internal pressure, D is the outside diameter of the pipe, t is the wall thickness, and η is the weld (or bond) joint factor which is equal to 1.0 for butt welded HDPE pipe. F in equation 6 is the axial force, A the cross-sectional area of the pipe, S_u is the ultimate tensile strength and SF is the safety factor. For the HDPE pipe used in this project, the long-term (50-year) strength is defined by test data as 1,600 psi at 70• F.

The first term of the left-hand side of equation 6 represents the stress induced in the longitudinal direction by Poisson's effect due to pressure in a restrained pipe. For HDPE, Poisson's ratio is 0.4, indicating that the magnitude of the term is only slightly less than the axial stress term of equation 2. A safety factor of 1.3 is recommended against this 50-year ultimate tensile strength. Comparing equations 2 and 6 indicates that the Antaki recommendation is slightly less conservative.

PEAK RESPONSES

As mentioned previously, calculations were performed for both ductile iron (DI) and High Density Polyethylene (HDPE) pipe and for a variety of soil properties and motion directions. The critical cases for determination of peak axial stress in the pipe loop occurred for the case of lower wave propagation velocity (2,000 fps) across the site and for directions parallel and perpendicular to the long leg of the pipe loop. The peak axial stress computed in the HDPE pipe from the seismic loading alone was of the order of 92 psi. The peak stress due to seismic, dead load and internal water pressure (using an operating pressure of 150 psi) was found to be about 730 psi in compression and 1,038 psi in tension. These values compare with the material allowables of 1,600 psi in compression and 3,200 psi in tension. The maximum stress in the HDPE pipe was found to occur at the intersection of the HDPE pipe with the DI pipe at the building interfaces. In addition, it was found that the influence of soil slippage along the pipes was small.

The stresses determined from the various computer runs were then compared with the capacity allowables defined above from the ASME Piping Code, including the effects of stress intensification factors for the various pipe fittings as well as the recommendations of Antaki (1997). It should be noted that in addition to the stress criteria, a strain criterion is also recommended to ensure against pipe wall wrinkling due to bending. In this case, bending strains are limited to values less than 0.4 * (t/d) where t is the wall thickness and d is the pipe diameter. For these pipe sizes, however, this strain allowable generally implies stresses much higher than that defined from the stress allowables. Therefore, the stress criteria were generally found to govern.

Finally, it was noted that for the case of HDPE pipe, the critical stresses were primarily controlled by peak axial stresses, with little effect of bending. For DI pipe, however, bending stresses were found to be more significant. In general, the seismic demand for the DI pipe (ratio of induced stress to allowable capacity) is higher than that for HDPE pipe. However, when comparing the effects of all loading including operating pressures, the HDPE has a somewhat higher peak demand/capacity ratio.

REFERENCES

"ADINA Theory and Modeling Guide", ADINA R&D Inc., Report ARD 95-8, February 1995.

"ADINA Verification Manual" ADINA R&D Inc. Report 95-9, February 1995.

"ASME Code for Pressure Piping B31", 1996

"Natural Phenomena Hazards Assessment Criteria", DOE Standard 1023-95, U.S. Department of Energy, September 1995

"Seismic Analysis of Safety Related Nuclear Structures and Commentary", American Society of Civil Engineers Standard 4, Draft Revision, September 1996

"Standard Review Plan", NUREG-0800, Office of Nuclear Reactor Regulation, U.S. Nuclear Regulatory Commission, Revision 2, 1989

Antaki, G. A., "Fire Loop Piping Criteria", PEC-SSA-97-0058, Westinghouse Savannah River Company, Aiken, SC, October 1997

Bathe, K. J., "Finite Element Procedures in Engineering Analysis", Prentice-Hall, Englewood Cliffs, NJ 1982

Costantino, C. J., Miller, C. A., Heymsfield, E., Yang, A., "CARES: Computer Analysis for Rapid Evaluation of Structures, Version

1.2", City University of New York for U.S. Nuclear Regulatory Commission, May 1996

Goen, L. K., "LANL Design Response Spectra", Report ESA-EA: 95-368, Los Alamos National Laboratory, July 1995

Goodling, E. C., "Flexibility Analysis of Buried Pipe", Report 79-PVP-82, ASME, 1982

Keller, M.D., "TA-55 Fire Loop", Letter Report Los Alamos National Laboratory, May 1997

TABLE 1 – BEST ESTIMATE SOIL PROPERTIES

Best Estimate Properties	Surface Fill	Weathered Tuff	Moderately Welded Tuff	Clean Sand Backfill
P-Wave Velocity (ft/sec)	1,000	1,800	4,000	1,313
S-Wave Velocity (ft/sec)	625	870	1,800	800
Unit Dry Density (pcf)	90.0	95.0	108.0	103.0
Elastic Modulus (ksi)	17.0	55.0	147.0	38.3
Shear Modulus (ksi)	7.6	20.0	62.0	14.2
Poisson's Ratio	0.33	0.33	0.18	0.35
Material Damping (%)	8.0	3.5	3.5	

TABLE 2 – ASSUMED VARIABILITY IN P-WAVE VELOCITY (fps)

	Surface Fill	Weathered Tuff	Moderately Welded Tuff	Sand Backfill
Best Estimate	1000	1800	4000	1313
Upper Bound	1300	2200	4600	1641
Lower Bound	800	1600	3000	985

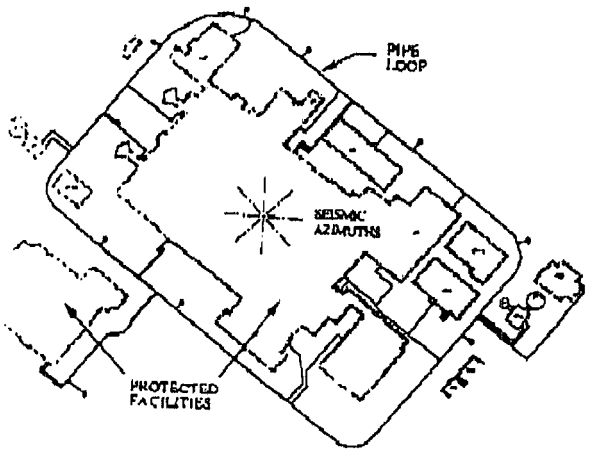

Figure 1 Schematic Diagram of Pipe Loop System and Protected Facilities

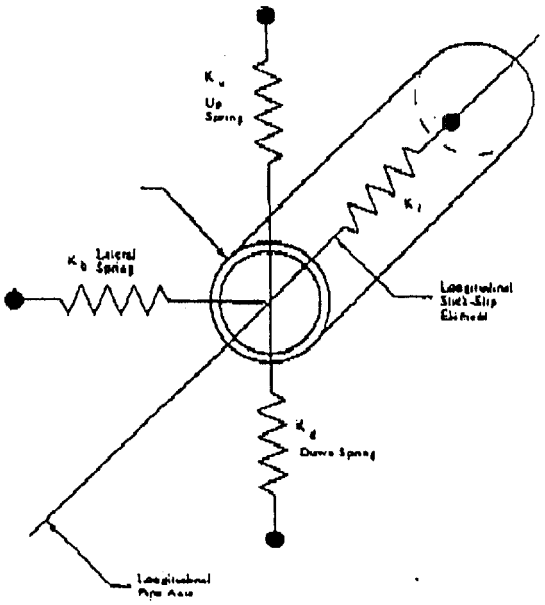

Figure 3 Soil-Structure Interaction Ground Spring Models at Pipe Nodes

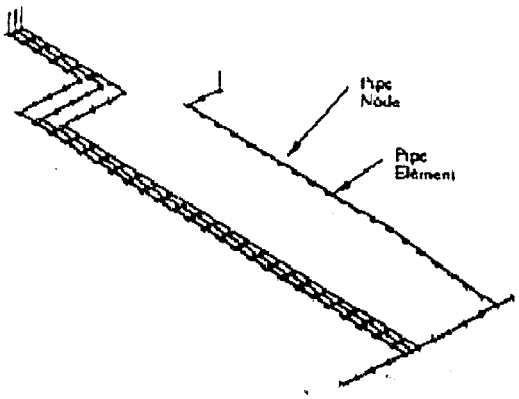

Figure 2 Typical Finite Element Beam/Mass Model of Pipe Elements

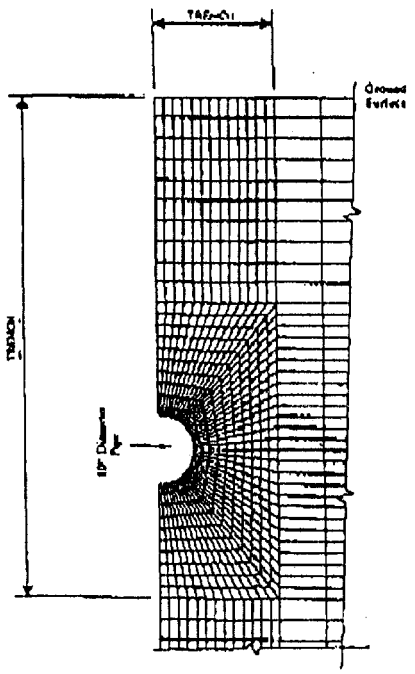

Figure 4 Static Finite Element Model Through Soil Pipe-Trench System for Transverse Stiffnesses

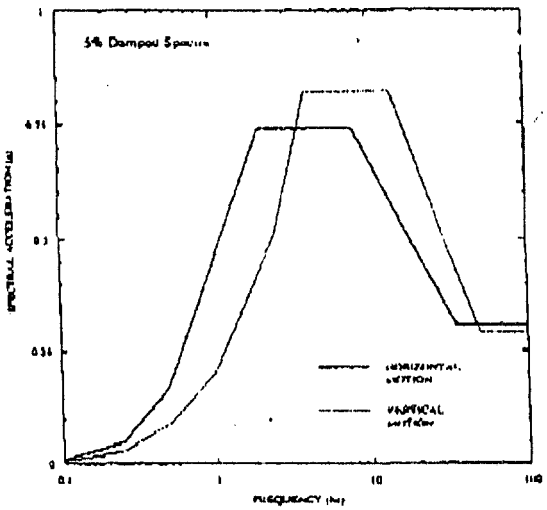

Figure 5 Criteria 5% Damped Response Spectra for Horizontal and Vertical Seismic Motions

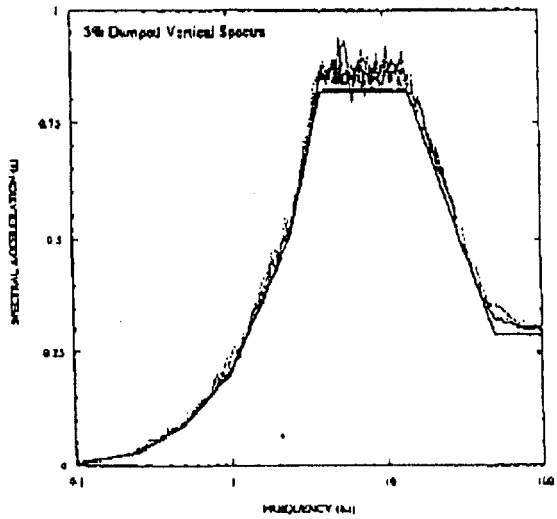

Figure 7 Comparison of Response Spectra from Artificial Ground Motions with Target Vertical Spectrum

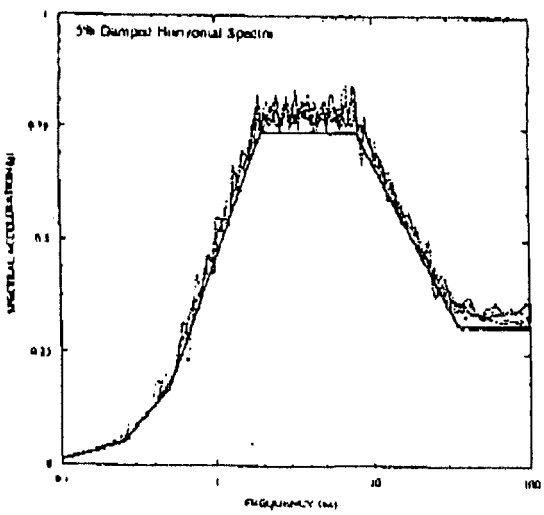

Figure 6 Comparison of Response Spectra from Artificial Ground Motions with Target Horizontal Spectrum

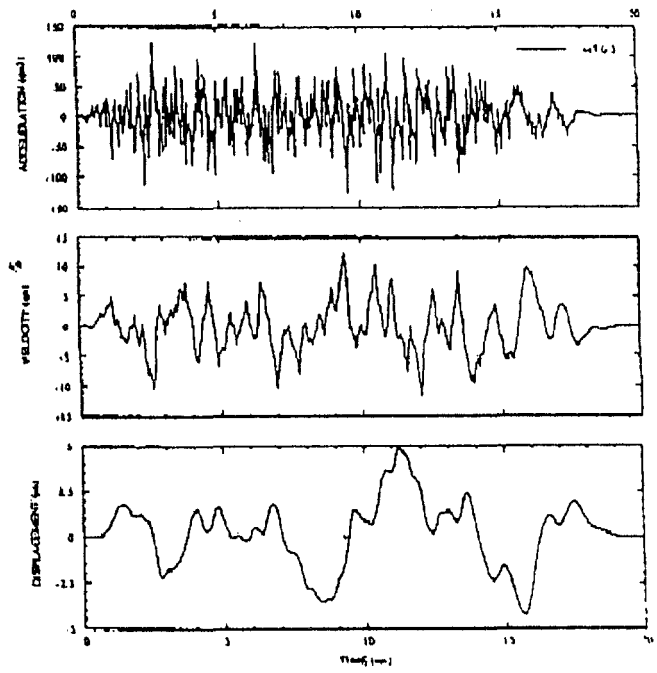

Figure 8 Typical Acceleration, Velocity and Displacement Histories for Artificial Ground Motion